Contrast's effect on spatial summation by macaque V1 neurons

Michael P. Sceniak[1], Dario L. Ringach[2], Michael J. Hawken[1] and Robert Shapley[1]

[1]*Center for Neural Science, New York University, 4 Washington Pl., New York, New York 10003, USA*

[2]*Departments of Neurobiology and Psychology, University of California Los Angeles, Los Angeles, California 90095, USA*

Correspondence should be addressed to M.P.S. (sceniak@cns.nyu.edu).

Stimulation outside the receptive field of a primary visual cortical (V1) neuron reveals intracortical neural interactions[1–6]. However, previous investigators implicitly or explicitly considered the extent of cortical spatial summation and, therefore, the size of the classical receptive field to be fixed and independent of stimulus characteristics or of surrounding context. On the contrary, we found that the extent of spatial summation in macaque V1 neurons depended on contrast, and was on average 2.3-fold greater at low contrast. This adaptive increase in spatial summation at low contrast was seen in cells throughout V1 and was independent of surround inhibition.

The nature of signal integration in space and time by neurons in the visual cortex is a fundamental problem in cortical physiology. There has been increasing interest in intracortical interactions among neurons outside the classical receptive field[1–3]. These interactions are important because they may form the neural basis for feature linking[5,6], contextual effects[4] and figure–ground modulation of neural responses[7]. Studies investigating these interactions usually distinguish between stimuli within the classical receptive field and those that fall on the 'surround' or outside the classical receptive field[4–7]. By measuring response as a function of stimulus area, we determined the spatial extent of the central region of the classical receptive field of a visual cortical cell at various contrasts. Preliminary estimates of spatial summation revealed surprising stimulus dependence, prompting the present investigation. We found that the extent of spatial summation shrinks at high stimulus contrast, suggesting a new view of cortical spatial summation.

Understanding the mechanism of contrast's effect on spatial summation requires dissecting contributions of central excitation from those of surround inhibition. For many cortical neurons, responses are inhibited by stimulation in the 'surround' of the receptive field[1–3]. One computational model[8] suggests that, at increased contrast, the surround grows relatively stronger, predicting the reduced spatial summation observed in a preliminary study of length summation in cat visual cortex (B. Jagadeesh & D. Ferster, *Soc. Neurosci. Abstr.* **16**, 130.11, 1990). To evaluate the role of the surround in contrast's modulation of spatial summation, we modified an analysis technique from retinal and cortical physiology and approximated the area–summation curves with a difference of Gaussians (DOG) model[9–11]. We found that increasing stimulus contrast decreased the size of the receptive-field center, but had little effect on surround suppression[5]. Our data suggest that contrast's modulation of receptive-field size involves changes of excitatory coupling between cortical cells.

Results

Area–summation curves for 85 cells were measured by stimulating each with circular patches of drifting sinusoidal gratings. We conducted length and width summation experiments on a subset ($n = 42$) of this population using rectangular patches varying in only one dimension. The spatial frequency, temporal frequency and orientation of the gratings were optimized in each case; responses were measured as a function of the patch radius, half-length or half-width. All cells increased responses as the size of the patch was increased from 0.1°. After initial summation, some cells showed response suppression (**Fig. 1a** and **b**), whereas others asymptoted (**Fig. 1c**). The optimal stimulus radius for spatial summation (indicated by arrows) was defined as the radius of the peak response (**Fig. 1a** and **b**) or, if there was no peak (**Fig. 1c**), the radius at which the response reached 95% of its asymptotic value. In all cells, optimal stimulus radius decreased as stimulus contrast increased.

Acquired area–summation curves were empirically fit with the difference of the integral of two Gaussians (see Methods and **Fig. 2a**). The narrower Gaussian is the excitatory, center mechanism and the broader Gaussian represents the surround mechanism. This function accurately captures the features of the summation curves (**Fig. 1**) and, under the assumption that the model is conceptually correct, allows one to separate the relative contributions of inhibition and excitation. The individual excitatory and inhibitory components (**Fig. 2b** and **c**) for the cell in Fig. 1a were compared, allowing us to estimate the space constant and gain of each Gaussian component.

The center of the difference of Gaussians (DOG) model characterizes the spatial envelope of sensitivity of the classical receptive field. The 'center' Gaussian can be treated as the envelope of the Gabor function that describes, approximately, the receptive field's sensitivity distribution[11,12]. Similarly, the 'surround' Gaussian overlapping the center mechanism can be thought of as the spatial envelope of sensitivity of a suppressive receptive field composed of several subregions[11,13]. As a first approximation, the model assumes that 'center' and 'surround' signals sum linearly. Additional nonlinear processes may describe the data even better. In terms of the DOG model, the main effect of contrast is on the excitatory space constant. As the DOG model provides a compact and accurate description of the data, we used it to

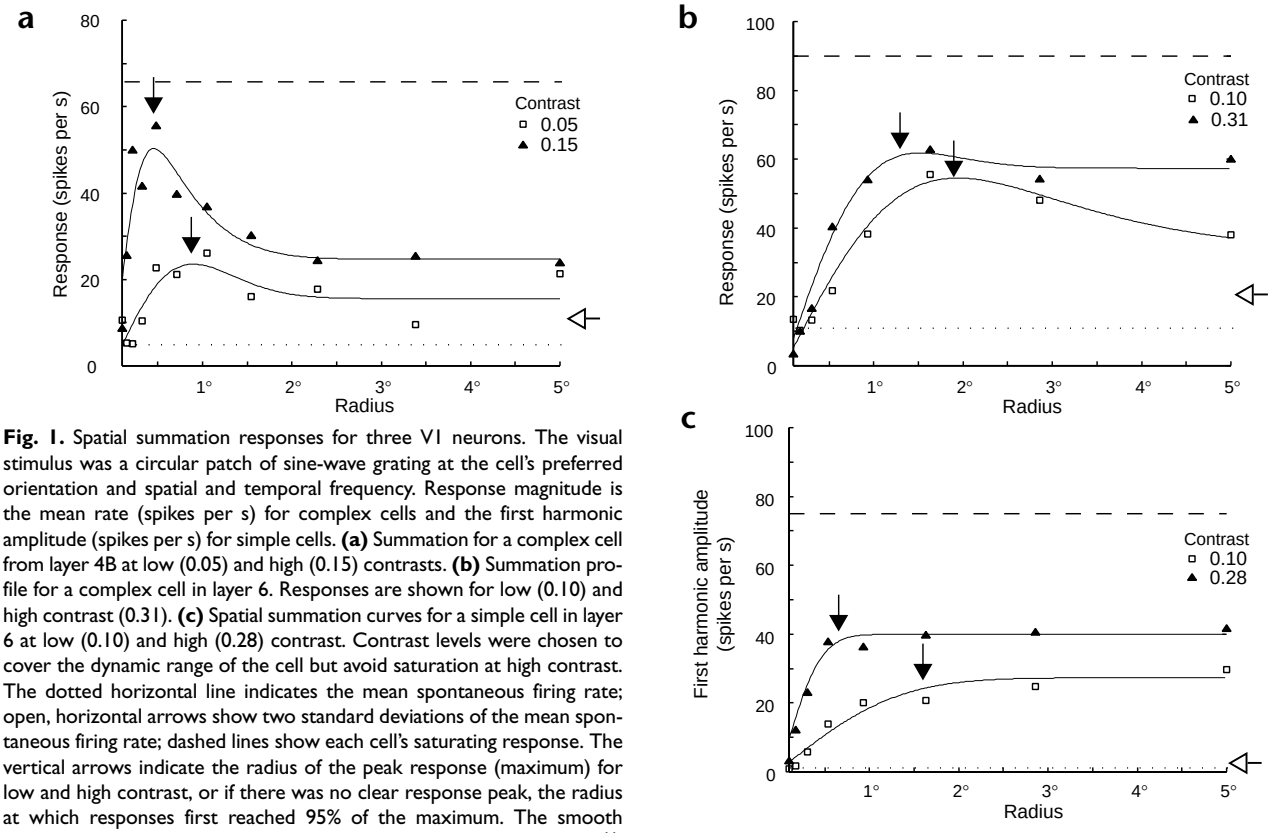

Fig. 1. Spatial summation responses for three V1 neurons. The visual stimulus was a circular patch of sine-wave grating at the cell's preferred orientation and spatial and temporal frequency. Response magnitude is the mean rate (spikes per s) for complex cells and the first harmonic amplitude (spikes per s) for simple cells. **(a)** Summation for a complex cell from layer 4B at low (0.05) and high (0.15) contrasts. **(b)** Summation profile for a complex cell in layer 6. Responses are shown for low (0.10) and high contrast (0.31). **(c)** Spatial summation curves for a simple cell in layer 6 at low (0.10) and high (0.28) contrast. Contrast levels were chosen to cover the dynamic range of the cell but avoid saturation at high contrast. The dotted horizontal line indicates the mean spontaneous firing rate; open, horizontal arrows show two standard deviations of the mean spontaneous firing rate; dashed lines show each cell's saturating response. The vertical arrows indicate the radius of the peak response (maximum) for low and high contrast, or if there was no clear response peak, the radius at which responses first reached 95% of the maximum. The smooth curves were fit to the data using the DOG model described in Methods[11].

infer possible neural mechanisms for spatial summation.

Separate examination of each parameter's contribution within the DOG model allows better appreciation of its influence on spatial summation. For a hypothetical response curve (solid curve, **Fig. 2d–f**) and a particular excitatory gain, K_e, we varied the value of the excitatory or inhibitory space constants, a or b, and/or the inhibitory gain, K_i, independently. As a was decreased with other parameters kept fixed, stimulus radius eliciting peak summation decreased, and responses declined more sharply for radii above and below this peak value. (**Fig. 2d**). Changing the space constant of inhibition strongly influenced the rate at which inhibition developed with radius, but did not change the radius of peak summation (**Fig. 2e**). Increasing the gain of inhibition, K_i, reduces the radius of peak summation, but the shift is modest and associated with strongly reduced responses (**Fig. 2f**). If excitation and inhibition, K_e and K_i, were increased proportionally as by an increase in contrast, the degree of shift in peak summation was negligible. Together, these simulations showed that the excitatory space constant, a, has the largest and clearest effect on the radius of peak summation. The value of a obtained from the low-contrast fit does not produce an acceptable fit to the high-contrast data containing a peak shift (data not shown); furthermore, no single values of a and b allow fits at both high and low contrast. Therefore, a must change when the peak shifts.

To quantify the contrast dependence of spatial summation, we estimated the excitatory space constant, a, at two contrast levels in each cell. These levels were near the low and high ends of the sloping region of the cell's contrast–response function. Strict criteria for stimulus contrast were used: responses to the low contrast were significantly greater than the spontaneous firing rate (two standard deviations or more), and high-contrast responses were below 90% of the saturating response. It was crucial to avoid response saturation that might yield spuriously low estimates of the center's excitatory space constant, a, if response amplitude saturated at small patch radius. The index of the contrast-dependent shift in the excitatory space constant, a, is the ratio of a at low to a at high contrast; a ratio greater than unity means that the excitatory space constant is greater at low than at high contrast. On average, this ratio was greater than unity for the entire population of cells (mean, 2.3; Wilcoxon test, $p < 0.001$; **Fig. 3d**) as measured with circular patch summation. We find similar results for length summation (mean, 2.7; **Fig. 3e**) and width summation (mean, 1.9; **Fig. 3f**).

The size of the classical receptive field has been typically estimated as the size of an optimal grating[4,11] or the length of an optimal-width bar[14] that elicits a maximal response. In order to confirm that the measures of receptive-field size estimated from the excitatory space constant, a, of the DOG model agreed with the classical estimates (arrows in **Fig. 1**), we compared them directly to show significant correlation ($r^2 = 0.75$, $p < 0.001$). Contrast-dependent changes in empirical receptive-field size also correlate with changes in a (**Fig. 4**). Therefore, contrast-dependent changes in a can account for most of the change observed in the optimal summation radius. The excitatory space constant is greater if measured with a low-contrast stimulus than if measured with a high-contrast stimulus for summation either over a circular patch or along the length or width dimension (**Fig. 3a–c**).

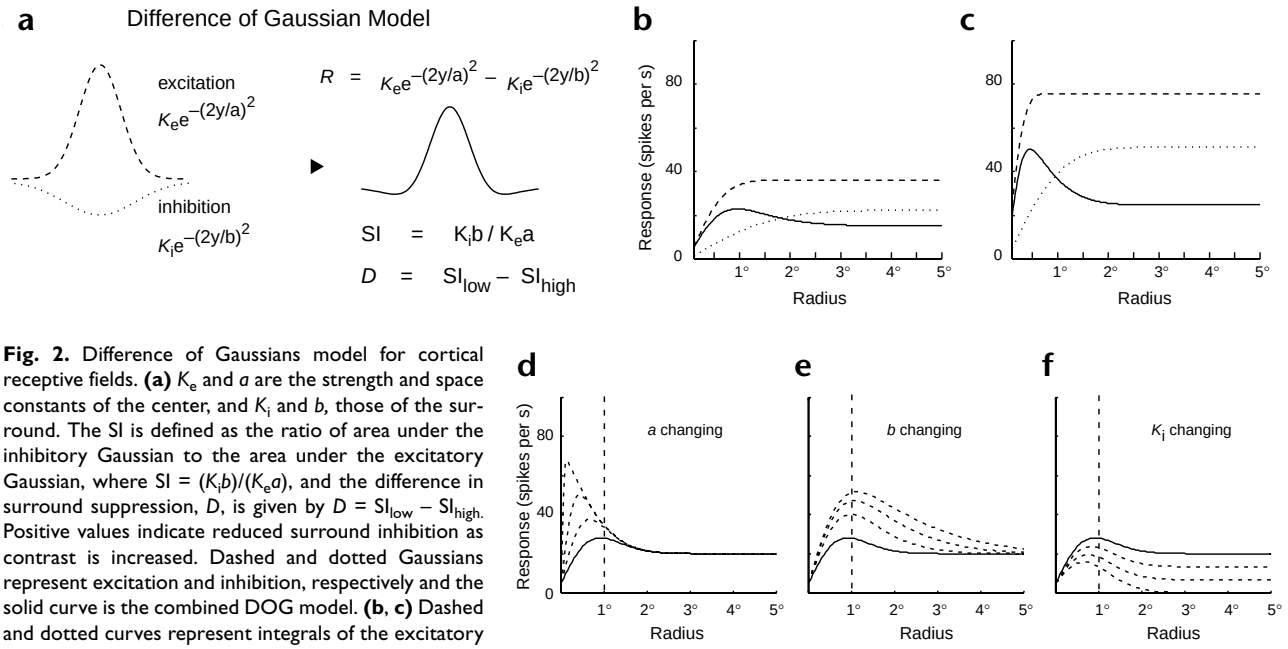

Fig. 2. Difference of Gaussians model for cortical receptive fields. **(a)** K_e and a are the strength and space constants of the center, and K_i and b, those of the surround. The SI is defined as the ratio of area under the inhibitory Gaussian to the area under the excitatory Gaussian, where $SI = (K_i b)/(K_e a)$, and the difference in surround suppression, D, is given by $D = SI_{low} - SI_{high}$. Positive values indicate reduced surround inhibition as contrast is increased. Dashed and dotted Gaussians represent excitation and inhibition, respectively and the solid curve is the combined DOG model. **(b, c)** Dashed and dotted curves represent integrals of the excitatory and inhibitory components and the solid curve the linear combination of these components that best fits the data. Solid curves were taken from the example in Fig. 1a. **(d–f)** Simulated changes in components of the DOG model. Solid curves show initial conditions preserved across examples d–f. **(d)** K_e, K_i and b are fixed as a is varied. Reduction in a produces a dramatic decrease in the summation peak. **(e)** K_e, K_i and a are fixed while b is increased. There is no decrease in the summation peak as b grows. **(f)** K_e, a and b are fixed as K_i increases. Increasing K_i produces modest decreases in peak summation.

Cells were assigned a cortical depth and layer by histological reconstruction of the electrode track (see Methods)[15]. Similar magnitude shifts in a were seen in both simple and complex cells of all cortical layers (**Fig. 5a**). This was also true for both length and width summation (**Fig. 5b**). Since the ratio a_{low}/a_{high} was ~1 for many cells and was broadly distributed, it is unlikely that the larger values of a_{low}/a_{high} derive from inherent properties of the LGN input.

Separately, we estimated the effect of contrast on surround suppression. After fitting the summation curves with the DOG function, we separated the excitatory and inhibitory Gaussian components and used the ratio of inhibitory to excitatory area,

$$SI = (K_i b)/(K_e a) \quad (1)$$

as a suppression index (SI; **Fig. 2a**). The difference between this ratio at low and high contrast,

$$D = (SI_{low} - SI_{high}), \quad (2)$$

is a measure of the change in surround suppression strength with contrast: positive values of D indicate less surround inhibition and negative values more surround inhibition at increased contrast.

The effect of contrast on surround suppression was variable. In 70% of the cells, the ratio of inhibition to excitation, SI, decreased with increasing contrast. However, in 30%, surround suppression increased as contrast increased. The change in surround suppression, D, was broadly distributed around a mean of +0.06 (**Fig. 6**). On average, surround strength seemed unaffected by contrast. The lack of consistent change in surround suppression strength with contrast makes it unlikely that contrast-dependent changes in surround suppression contributed to the observed changes in the excitatory space constant with contrast. Nevertheless, we confirmed a lack of significant correlation ($r^2 = 0.2$) between D and the change in the excitatory space constant with contrast (a_{low}/a_{high}). Although change in the strength of inhibition ($K_i b/K_e a$) is not correlated with the change in optimal summation, there is probably a concomitant change in the space constant of inhibition, b, with changes in the excitatory space constant. Because the individual parameters K_i and b were not independently constrained in our fits, we consider only the product, $K_i b$, which is well constrained.

Comparing the area–response curve in Fig. 1 with our estimates of a_{low}/a_{high} and D allows us to gain some intuition about the relationship between the DOG model and the actual data. For the neuron in Fig. 1a, the excitatory space constant ratio a was 2.62; in Fig. 1b, it was 1.48 and in Fig. 1c, 2.54. For the same cells, the change in the ratio of surround to center strength varied with contrast: in Fig. 1a, $D = 0.03$; in Fig. 1b, $D = 0.02$ and in Fig. 1c, $D = 0$. Note that the increase in surround-to-center ratio at high contrast was negligible in Fig. 1a ($D = 0.03$), whereas the center size shrank with increasing contrast by a factor of 2.62.

Cases in which the excitatory space constant changed but inhibition remained weak support the idea that a changes independent of inhibition. For a subpopulation with SI_{low} and SI_{high} less than 0.3 ($n = 11$, **Fig. 7a**), the excitatory space constant ratio (a_{low}/a_{high}) follows the trend observed for the entire population (mean, 2.7; **Fig. 7b** and **c**). The change in the inhibitory strength, D, with contrast is not significant for any of these cells.

Discussion

The envelope for stimulus summation in cortical cells appears to shrink as contrast is increased. At threshold, detection of sig-

nals by cells with different receptive-field areas should be proportional to the square of the excitatory space constant, a^2:

$$\text{contrast sensitivity} = (\text{contrast gain})(a^2). \quad (3)$$

Therefore, for a given contrast gain, the 2.3-fold average increase in receptive-field center radius at low contrast would require sensitivity to low-contrast stimuli to be $(2.3)^2$-fold greater than if the receptive-field size were the same as at high contrast. Similarly, localization sensitivity at a given contrast can be defined as the slope of the radius–summation curve midway between zero and the radius of peak summation. When the width of the summation curve is reduced at high contrast, the slope will increase, proportionally increasing localization sensitivity. The visual system thus achieves improved sensitivity at low contrast and improved localization at high contrast. Based on our observations, one can conclude that the visual cortex accomplishes this task by altering the spread of excitation independent of surround suppression.

Our results are strong evidence that the receptive field is not size invariant, but depends on stimulus conditions. Others have challenged the static nature of receptive-field size, but the results and conclusions of earlier studies were not completely convincing. Dynamic context-dependent changes in receptive-field size have been reported in cat visual cortical neurons after stimulating with an artificial scotoma. However, others have failed to reproduce these results, finding a change in response gain but no measurable change in the receptive-field size[17]. Another study claimed to see contrast-dependent changes in spatial summation similar to those reported here[18]. However, because this report included areal summation data from only one cat cortical cell, it is difficult to judge the magnitude and generality of the phenomenon. A preliminary report on length summation in cat cortical cells showed summation changes with contrast that resemble our data on monkey cortical neurons (B. Jagadeesh & D. Ferster, *Soc. Neurosci. Abstr.* **16**, 130.11, 1990), but these results may result from saturation of response amplitude at high contrast. It has been shown that flanking inhibition is reduced by lowering contrast of a central stimulus[5]. These findings are consistent with increased spread of excitation along the length dimension under low-contrast stimulation, but one cannot distinguish this possibility from response facilitation independent of a spatial change in excitation. However, our findings of receptive-field size variation with contrast demonstrate robustly and significantly increased spread of excitation under low-contrast stimulation.

One inhibition model used to account for decreased spatial summation at high contrast requires surround suppression to increase with increasing contrast[8]. However, we found no correlation between contrast-dependent changes in the excitatory space constant and SI in monkey V1. Explanation of our data requires

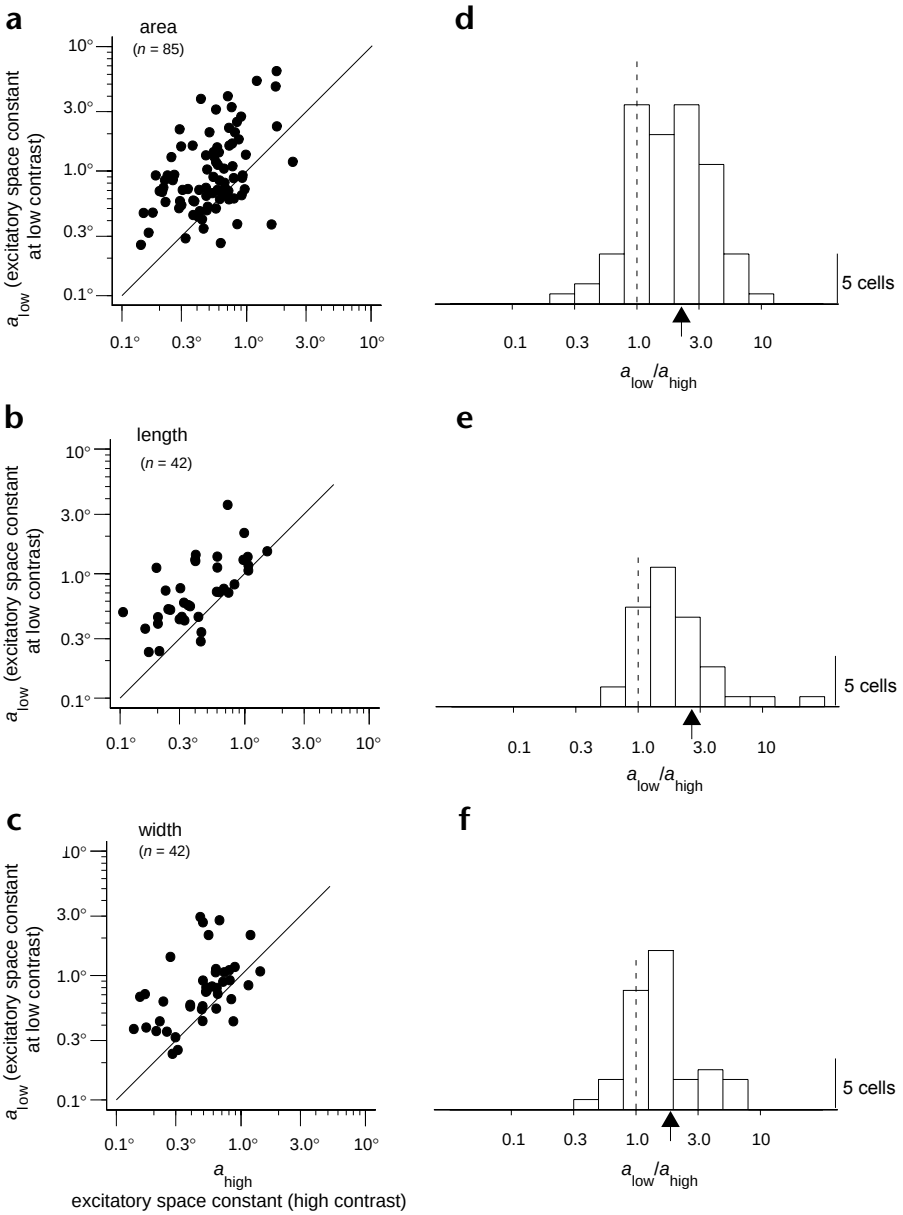

Fig. 3. Dependence of excitatory spread on stimulus contrast. **(a–c)** Scatter plot of excitatory space constant parameter at high versus low contrast measured for circular patch summation, length summation and width summation respectively. **(d–f)** Histogram of the entire population, showing the ratio (a_{low}/a_{high}) of the excitatory spread at low to high contrast for each cell for area, length and width summation respectively. A value greater than unity indicates that the excitatory space constant is smaller when measured with high contrast stimuli. The arrow indicates the population average.

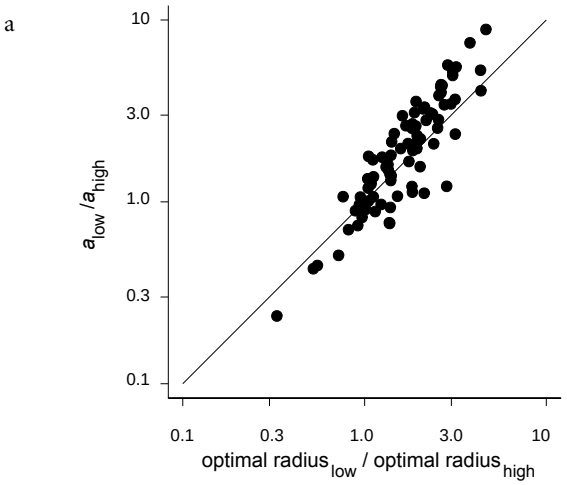

Fig. 4. Comparison of contrast-dependent change in excitatory space constant, *a*, and optimal radius. Changes in either excitatory space constant or the empirical optimal radius are defined as the ratio of their estimates at low to high contrast. The excitatory space constant *a* is derived from the difference of Gaussians model. Optimal radius values are empirical estimates from either the peak or asymptotic value of the fitted summation curves.

mechanism that is independent of surround suppression. One possible mechanism involves contrast modulation of lateral excitation from cortical connections.

The cellular and/or network basis for the effect of contrast on corticocortical excitation must increase the excitatory space constant at low contrast and decrease it at high contrast independent of surround suppression. We hypothesize that, under conditions of low contrast stimulation, lateral excitatory connections between cortical neurons with spatially nonoverlapping receptive fields are strong. This lateral coupling enhances spatial pooling of their receptive fields and increases the effective size of the central receptive field. As the input signal increases, lateral connections are weakened and spatial pooling is similarly reduced. One cellular mechanism for changing lateral coupling is depression of excitatory corticocortical synapses at higher levels of mean activity caused by higher contrast[19–21]. Another possibility is the increased shunting of lateral EPSPs resulting from tonic inhibition elicited by increased cortical activity at higher contrast[22–25]. For both hypothetical mechanisms, signals from farther away requiring polysynaptic transmission would undergo greater attenuation when mean cortical activity increased. Whatever the mechanism, it is clear that the cortex can rapidly adapt spatial summation; it is not a fixed, passive filter of the visual scene.

Reduction of spatial integration at high contrast makes functional sense. A strong signal created by a high-contrast stimulus gives the cortex the ability to spatially localize image features. At low contrast, localization is sacrificed to achieve the high sensitivity and better detection capabilities provided by greater spatial summation. The adaptive change of spatial signal summation with contrast allows the visual system to optimize performance under changing stimulus conditions.

The effect of contrast on cortical receptive-field size is also relevant to our understanding of cortical contrast gain control[13,26,27], and to cortical adaptation in general. Previous models of cortical contrast gain control[25] shared one salient feature with accounts of center–surround interaction in cortex—both assumed that spatial summation within the conventional receptive field was invariant with stimuli or context. Thus, they assumed a fixed spatial input to the cortical cell that could be modulated in amplitude or time course. On the contrary, one adaptation to high contrast was shrinkage in the extent of cortical spatial summation in the conventional receptive field. Therefore, contrast adaptation involves more functional reorganization of the cortex than was conceived in previous theories.

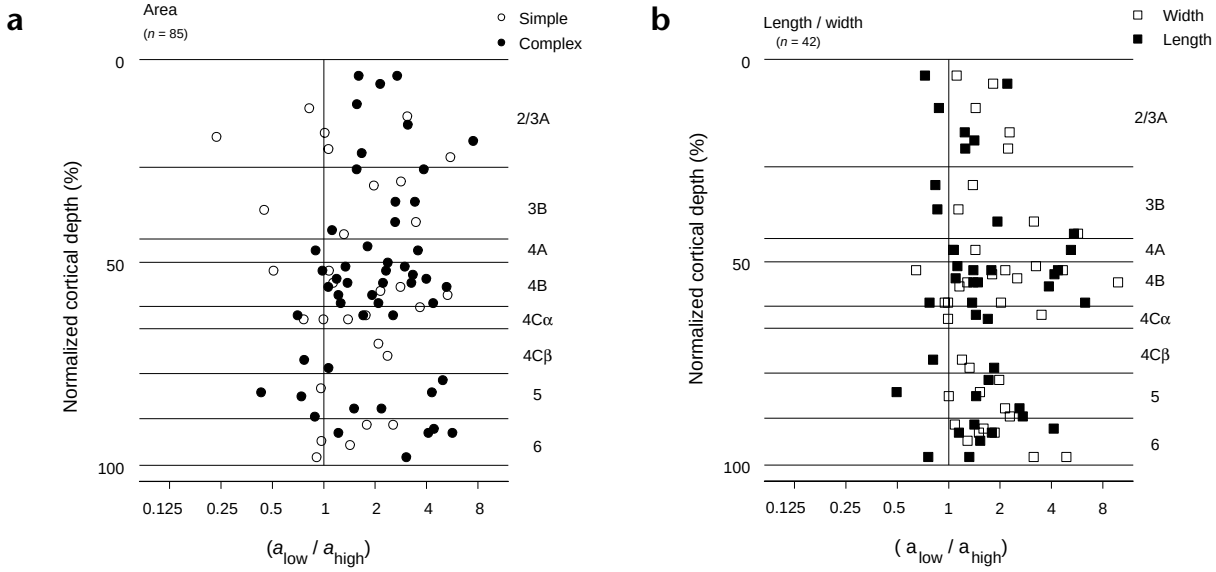

Fig. 5. Laminar distribution of changes in excitatory space constant with contrast. **(a)** Ratio of excitatory space constants for circular patch area summation at low contrast to constant at high contrast (a_{low}/a_{high}) in simple or complex cells across cortical layers. **(b)** Cortical distribution of fractional change in length (■) and width summation (□). Cortical layering is based on histological reconstruction of the electrode penetration and is represented here as the normalized cortical depth along with the anatomical label[15,29,30].

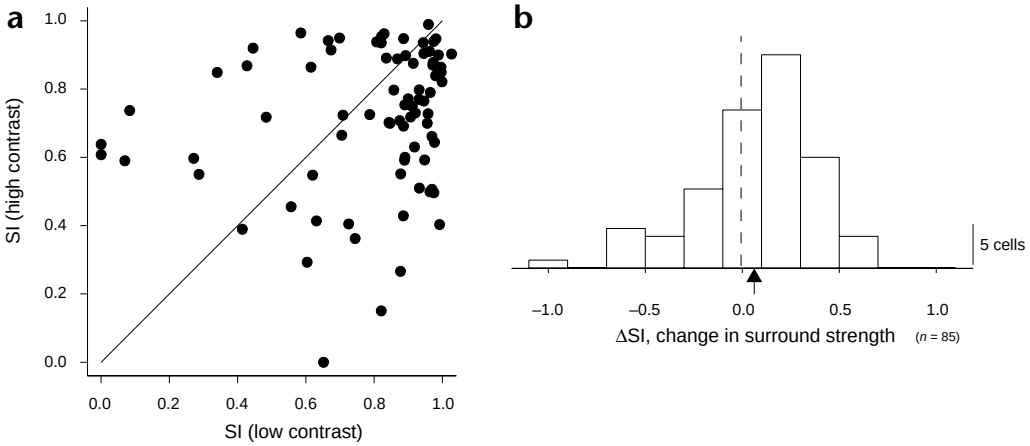

Fig. 6. Changes in surround strength with contrast. **(a)** Suppression index (SI) estimates compared for low versus high stimulus contrast. **(b)** Histogram for the values of $D = SI_{low} - SI_{high}$ within each cell across the population of cells for which circular area summation experiments were performed (n = 85). The arrow indicates the population average (0.06).

METHODS

We recorded extracellularly from 130 neurons in parafoveal primary visual cortex of anesthetized (sufentanil citrate, 6 µg per kg per h) and paralyzed (pancuronium bromide, 0.1 mg per kg per h) adult old-world monkeys (*Macaca fascicularis*). Electrocardiogram and expired CO_2 were continuously monitored and blood pressure was measured noninvasively. All procedures conformed to guidelines approved by the New York University Animal Welfare Committee. Single unit recordings were made with glass-coated tungsten microelectrodes with 5–15-µm tips[28]. Spikes were detected using a Bak (Maryland, USA) DDIS-I dual window discriminator and were time-stamped with an accuracy of 1 ms using a CED-1401 Plus (Cambridge, UK) data acquisition system. Strict criteria for single-unit recording included fixed shape of the action potential and the absence of spikes during the absolute refractory period. Small electrolytic lesions (2–3 µA for 2–3 s) were made along the length of each penetration; details of the reconstruction of the penetrations and assignment of cells to cortical layers are described in ref. 15.

Visual stimuli were generated on a Silicon Graphics O2 computer and displayed on a Sony Multiscan 17se II color monitor operating at 100-Hz frame refresh. The mean luminance of the display was 56 cd per m^2. The screen measured 24 cm high by 34 cm wide and was viewed at a distance of 115 cm.

Before the spatial summation experiment was conducted, each cell was characterized to determine its preference for orientation, spatial frequency and temporal frequency tuning as well as its contrast response function. The optimized values for these parameters were used in the summation experiment. After these initial experiments, the center of the receptive field was carefully located using a small (diameter, 0.2°) circular grating patch. Once the center was located, circular patches of drifting sinusoidal grating centered over the receptive field were presented. Each grating patch size was presented for four seconds. Four-second blanks of the same mean luminance as the grating stimuli were presented interleaved with grating stimuli in order to determine the spontaneous firing rate and to avoid response adaptation. The patch sizes were presented in a random order. The radius ranged from 0.1° to 5° of visual angle in logarithmic steps. Each summation curve consisted of 10 radii with 2 repeats at each size. Contrast levels were held constant during repeats to avoid effects of adaptation. Outside each patch, the rest of the screen (12° by 17°, visual angle) was kept at the mean luminance of 56 cd per m^2.

We performed this procedure at two contrast levels. The contrast levels chosen were taken from the linear region of the contrast response function of each cell. Therefore, the contrast levels are chosen based on the cell's response. Low contrasts were chosen such that they were near the low end of the contrast response function, but elicited responses that were significantly greater than the spontaneous firing rate (2 standard deviations or more). High contrasts were selected to elicit responses that were less than 90% of the saturation response for each cell.

We repeated the summation experiment using rectangular patches whose length or width was varied randomly in the same manner described above for the circular patches. Therefore, we acquired area, length and width summation curves at two contrast levels in three temporally separated experiments.

Each summation curve was fitted using the following empirical function:

$$R(s) = R_0 = K_e \int_{-s/2}^{s/2} e^{-(2y/a)^2} dy - K_i \int_{-s/2}^{s/2} e^{-(2y/b)^2} dy \qquad (4)$$

Here, R_0 is the spontaneous rate, and each integral represents the relative contribution from putative excitatory and inhibitory components

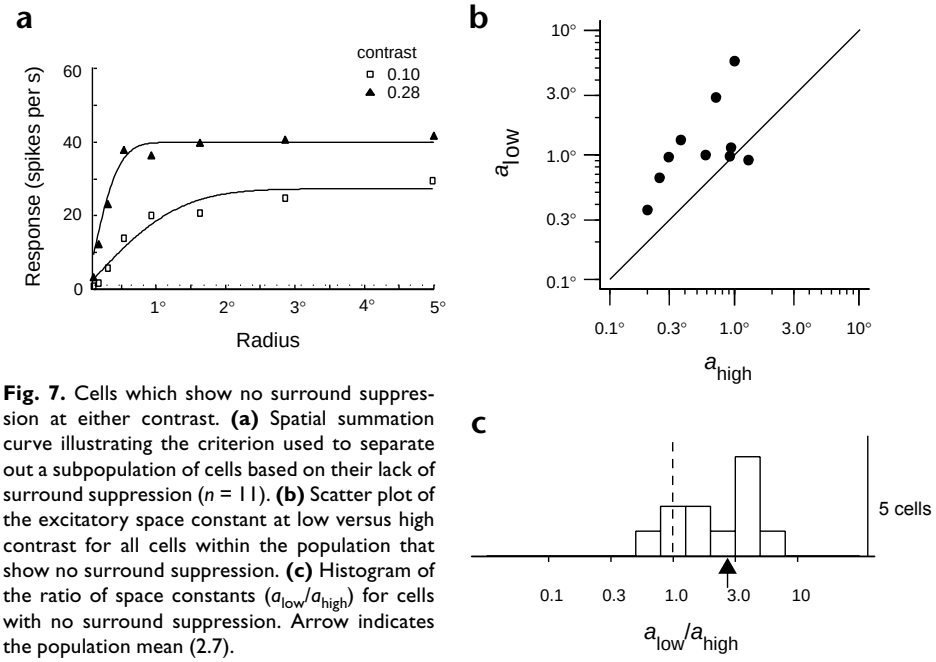

Fig. 7. Cells which show no surround suppression at either contrast. **(a)** Spatial summation curve illustrating the criterion used to separate out a subpopulation of cells based on their lack of surround suppression (n = 11). **(b)** Scatter plot of the excitatory space constant at low versus high contrast for all cells within the population that show no surround suppression. **(c)** Histogram of the ratio of space constants (a_{low}/a_{high}) for cells with no surround suppression. Arrow indicates the population mean (2.7).

respectively[11]. Values of K_e, a, K_i and b were optimized to provide the best MSE fit to the data. Excitatory space constant measures are taken as the parameter a from the fitted curves for the first harmonic response of simple cells and the DC response of complex cells. A suppression index measure was also estimated from the fitted curves. This measure is the ratio of area under the inhibitory Gaussian over that of the excitatory Gaussian ($K_i b/K_e a$).

Acknowledgements

We thank Shasta Sabo and Haim Sompolinsky for their comments. Lorraine Smith assisted in the histological reconstruction and during physiology experiments. This work was supported by National Institute of Health grants EY01472 and EY08300 and Sloan Foundation Grant in Theoretical Neuroscience 97-12-3.

RECEIVED 2 MARCH; ACCEPTED 2 JUNE 1999

1. Maffei, L. & Fiorentini, A. The unresponsive regions of visual cortical receptive fields. *Vision Res.* **16**, 1131–1139 (1976).
2. Nelson, J. I. & Frost, B. J. Orientation-selective inhibition from beyond the classic visual receptive field. *Brain Res.* **139**, 359–365 (1978).
3. Allman, J., Miezin, F. & McGuinness, E. Stimulus specific responses from beyond the classical receptive field: neurophysiological mechanisms for local-global comparisons in visual neurons. *Annu. Rev. Neurosci.* **8**, 407–430 (1985).
4. Levitt, J. B. & Lund, J. S. Contrast dependence of contextual effects in primate visual cortex. *Nature* **387**, 73–76 (1997).
5. Polat, U., Mizobe, K., Pettet, M. W., Kasamatsu, T. & Norcia, A. M. Collinear stimuli regulate visual responses depending on cell's contrast threshold. *Nature* **391**, 580–584 (1998).
6. Kapadia, M. K., Ito, M., Gilbert, C. D. & Westheimer, G. Improvement in visual sensitivity by changes in local context: parallel studies in human observers and in V1 of alert monkeys. *Neuron* **15**, 843–856 (1995).
7. Zipser, K., Lamme, V. A. & Schiller, P. H. Contextual modulation in primary visual cortex. *J. Neurosci.* **16**, 7376–7389 (1996).
8. Somers, D. C. *et al.* A local circuit approach to understanding integration of long-range inputs in primary visual cortex. *Cereb. Cortex* **8**, 204–217 (1998).
9. Rodieck, R. W. Quantitative analysis of cat retinal ganglion cell response to visual stimuli. *Vision Res.* **5**, 583–601 (1965).
10. Enroth-Cugell, C. & Robson, J. G. The contrast sensitivity of retinal ganglion cells of the cat. *J. Physiol. (Lond.)* **187**, 517–552 (1966).
11. DeAngelis, G. C., Freeman, R. D. & Ohzawa, I. Length and width tuning of neurons in the cat's primary visual cortex. *J. Neurophysiol.* **71**, 347–374 (1994).
12. Palmer, L. A. & Davis, T. L. Receptive-field structure in cat striate cortex. *J. Neurophysiol.* **46**, 260–276 (1981).
13. Bonds, A. B. Role of inhibition in the specification of orientation selectivity of cells in the cat striate cortex. *Vis. Neurosci.* **2**, 41–55 (1989).
14. Sillito, A. M., Grieve, K. L., Jones, H. E., Cudeiro, J. & Davis, J. Visual cortical mechanisms detecting focal orientation discontinuities. *Nature* **378**, 492–496 (1995).
15. Hawken, M. J., Parker, A. J. & Lund, J. S. Laminar organization and contrast sensitivity of direction- selective cells in the striate cortex of the Old World monkey. *J. Neurosci.* **8**, 3541–3548 (1988).
16. Pettet, M. W. & Gilbert, C. D. Dynamic changes in receptive-field size in cat primary visual cortex. *Proc. Natl. Acad. Sci. USA* **89**, 8366–8370 (1992).
17. DeAngelis, G. C., Anzai, A., Ohzawa, I. & Freeman, R. D. Receptive field structure in the visual cortex: does selective stimulation induce plasticity? *Proc. Natl. Acad. Sci. USA* **92**, 9682–9686 (1995).
18. Sengpiel, F., Sen, A. & Blakemore, C. Characteristics of surround inhibition in cat area 17. *Exp. Brain Res.* **116**, 216–228 (1997).
19. Markram, H. & Tsodyks, M. Redistribution of synaptic efficacy: a mechanism to generate infinite synaptic input diversity from a homogeneous population of neurons without changing absolute synaptic efficacies. *J. Physiol. (Paris)* **90**, 229–232 (1996).
20. Thomson, A. M. Activity-dependent properties of synaptic transmission at two classes of connections made by rat neocortical pyramidal axons in vitro. *J. Physiol. (Lond.)* **502**, 131–147 (1997).
21. Thomson, A. M. & Deuchars, J. Synaptic interactions in neocortical local circuits: dual intracellular recordings in vitro. *Cereb. Cortex* **7**, 510–522 (1997).
22. Bernander, O., Douglas, R. J., Martin, K. A. & Koch, C. Synaptic background activity influences spatiotemporal integration in single pyramidal cells. *Proc. Natl. Acad. Sci. USA* **88**, 11569–11573 (1991).
23. Häusser, M. & Clark, B. A. Tonic synaptic inhibition modulates neuronal output pattern and spatiotemporal synaptic integration. *Neuron* **19**, 665–678 (1997).
24. Hirsch, J. A., Alonso, J. M., Reid, R. C. & Martinez, L. M. Synaptic integration in striate cortical simple cells. *J. Neurosci.* **18**, 9517–9528 (1998).
25. Borg, G. J., Monier, C. & Frégnac, Y. Visual input evokes transient and strong shunting inhibition in visual cortical neurons. *Nature* **393**, 369–373 (1998).
26. Ohzawa, I., Sclar, G. & Freeman, R. D. Contrast gain control in the cat's visual system. *J. Neurophysiol.* **54**, 651–667 (1985).
27. Carandini, M. & Heeger, D. J. Summation and division by neurons in primate visual cortex. *Science* **264**, 1333–1336 (1994).
28. Merrill, E. G. & Ainsworth, A. Glass-coated platinum-plated tungsten microelectrodes. *Med. Biol. Eng.* **10**, 662–672 (1972).
29. Lund, J. S., Hendrickson, A. E., Ogren, M. P. & Tobin, E. A. Anatomical organization of primate visual cortex area V1. *J. Comp. Neurol.* **202**, 19–45 (1981).
30. Callaway, E. M. Local circuits in primary visual cortex of the macaque monkey. *Annu. Rev. Neurosci.* **21**, 47–74 (1998).